Imaging system for hypervelocity dust injection diagnostic on NSTX

L. A. Dorf,[a] A. L. Roquemore,[b] G. A. Wurden, C. M. Ticos, and Zhehui Wang
Los Alamos National Laboratory, Los Alamos, New Mexico 87545

(Received 6 May 2006; presented on 8 May 2006; accepted 24 July 2006; published online 10 October 2006)

The novel hypervelocity dust injection diagnostic will facilitate our understanding of basic aspects of dust-plasma interaction and magnetic field topology in fusion plasma devices, by observing "comet tails" associated with the injected micron-size dust particles. A single projection of the tail onto an image plane will not provide sufficient information; therefore, we plan to use two views, with intensified DiCam-Pro cameras on two NSTX ports. Each camera can furnish up to five overlaying sequential images with gate times greater than 3 ns and 1280×1024 pixel resolution. A coherent fiber bundle with 1500×1200 fibers will relay the image from an imaging lens installed directly on the port to the camera optics. The lens receives light from the outer portion of the NSTX cross section and focuses a 1 cm tail onto at least 60 fibers for adequate resolution. The estimated number of photons received by the camera indicates signal-to-noise ratios of 10^2-10^4, with the use of a 10 nm bandwidth filter. The imaging system with one camera was successfully tested on NSTX in 2005. Photographing lithium pellets yielded bright and distinctive pictures of the tails nearly aligned with *B* lines. We also observed that the bright "filaments"—plasma cords with high density and temperature—are present in both top and bottom portions of the machine. © *2006 American Institute of Physics.* [DOI: 10.1063/1.2336790]

I. INTRODUCTION

Imaging cameras have been employed on ASDEX, TFTR, C-Mod, JET, and other plasma experiments.[1–9] On NSTX and other tokamaks, these systems have been used to examine plasma wall interaction and macroscopic phenomena in the bulk plasma or divertor regions. Striation angle measurements have been utilized to infer plasma *q* profiles.[10] Comprehensive studies of pellet ablation clouds were also performed.[1] Wide optical views are typically adequate for these tasks, where ultrahigh spatial resolution is not required.

The imaging system for our novel hypervelocity dust injection (HDI) diagnostic should be able to simultaneously detect ten or more optical tails associated with dust plumes.[11–13] For micron-size dust particles, the plumes are expected to be not more than 1 cm long (for pellet ablation clouds this number can be from several to several tens of centimeters). The tails are expected to be aligned with local magnetic field vectors inside the NSTX plasma. The particles will be injected with the velocities of the order of 1–10 km/s. A 100 ns gated exposure is therefore required to freeze motion effects. The number of visible photons per pixel accumulated in the change-coupled device (CCD) during one exposure needs to be sufficient to produce an adequately defined image, and filters can be used to reduce plasma background light, as necessary. This forms the basis for the dust imaging system design.

A prototype imaging system with an intensified DiCam Pro camera (Fig. 1) was successfully tested on NSTX. Photographing lithium pellets yielded bright and distinctive pictures of the tails nearly aligned with *B* lines.

II. DUST IMAGING SYSTEM DESIGN

To achieve adequate spatial and temporal resolution, we plan to use an intensified DiCam Pro imaging camera[8] (Cooke Corporation). The camera can furnish up to five overlaying sequential images with gate times greater than 3 ns and 1280×1024 pixel resolution. To minimize the influence of NSTX magnetic fields, the camera will be placed inside an iron enclosure several meters from the machine. A

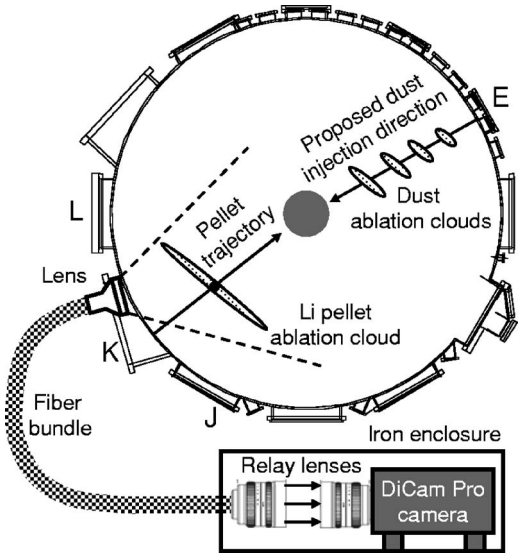

FIG. 1. A prototype imaging system with intensified DiCam Pro camera tested on NSTX in 2005 by observing lithium pellets ablation clouds.

[a]Electronic mail: ldorf@lanl.gov
[b]Also at the Princeton Plasma Physics Laboratory, Princeton, NJ 08543.

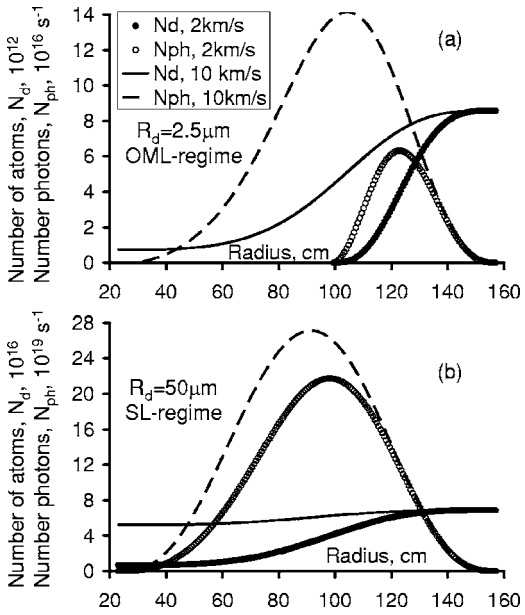

FIG. 2. Estimated number of atoms remaining in the carbon dust particle and number of photons emitted per second due to ablation vs particle's radial position inside NSTX for two particle velocities.

coherent fiber bundle with 1500×1200 10×10 μm^2 fibers[21] (Schott Fiber Optics, Inc.) will relay the image from an imaging lens installed directly on the port to the camera optics. A 36×24 mm^2 rectangular image obtained from a 35 mm format lens will overfill the 15×11 mm^2 fiber bundle by about two times. Therefore, to survey the outer portion ($\sim1/2$) of the NSTX cross section, the field of view of the imaging lens should be such that the lens could collect light from the entire cross section. A minimum object distance for the lens should be about 25–30 cm. Since the position of a dust particle inside the plasma at the time of exposure varies, a variable focus (zoom) lens needs to be employed. For a lens with a depth of field of several to several tens of centimeters (which is typical for commercially available lenses at maximum aperture setting), this will allow a dust tail with a cross section of a few millimeters and a length of 1 to a few centimeters to be always in focus at the time of exposure, and the image of the tail to be sufficiently large for obtaining a high-resolution picture.

To filter out the background light from the NSTX plasma, a narrow-band ($\sim$10 nm wide) interference filter can be placed between the fiber bundle and the camera (i.e., in the parallel beam of light between two image relay lenses in Fig. 1). The most dominant visible spectral lines for C I and C II are 426.7, 538, 601.3, and 657.8 nm, and for Li I and Li II they are 548.4, 548.6, and 670.8 nm, which determines the selection of the filter.

To estimate how deep a dust particle can penetrate into the NSTX plasma and the number of photons emitted per second due to ablation, we developed a time-dependent dust charging model.[14] Unlike a recent dust-particle transport model by Pigarov *et al.*,[15] for example, our model considers time evolution of the particle surface charge without assuming a floating potential at the particle surface, and works in both orbital motion limited (OML) or sheath limited (SL)

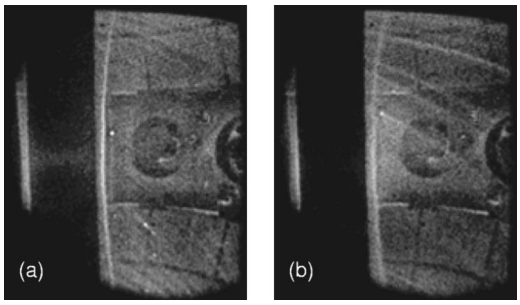

FIG. 3. Plasma filaments observed during shots 116056 (a) and 116059 (b) are present in both top and bottom portions of NSTX. Exposure=25 μs, delay=200 ms (a) and 150 ms (b).

regimes,[16] i.e., for different relations between the particle radius and the Debye length. We assumed that a thick ablation cloud typical for pellets is not formed for dust. We also assumed that each sublimed atom is ionized once and on average and simplistically emits one photon. Figure 2 shows the results of numerical simulations for a carbon dust particle. We used $T_i\approx T_e$, $T_e=T_{e0}[1-(r/a)^2]^{1.5}$, and $n_e=n_{e0}[1-(r/a)^2]^{0.5}$, where $T_{e0}=1000$ eV is the peak electron temperature, $n_{e0}=5\times10^{13}$ cm^{-3} is the peak plasma density, $a=67$ cm is the minor radius, and $r=R-R_0$ is the particle's radial position relative to the major radius, $R_0=90$ cm.[17–19]

Using Fig. 2(a), the maximum number of photons received by the lens during a 100 ns exposure can now be estimated as $N_{ph}^{tot}\sim1.4\times10^{10}\,\Omega$, where $\Omega=(D/4S)^2$ is the ratio between the solid angle of the lens and 4π, D is the

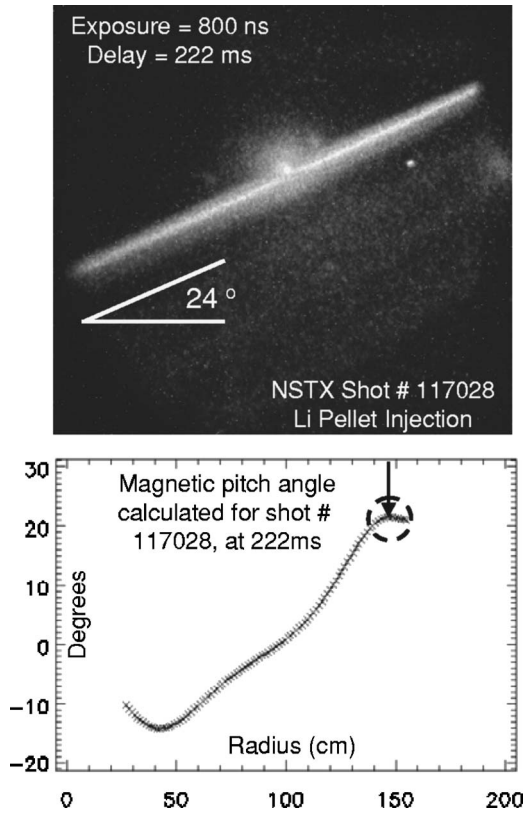

FIG. 4. Pitch angle calculation from EFIT_02 program corresponds closely to the measured value for Li pellet ablation cloud. The circle represents error bars for the pellet's radial position and calculated pitch angle.

diameter of the lens, and S is the distance between the lens and the dust particle. For $D=5$ cm and $S=50$ cm, we have $\Omega=6.25\times10^{-4}$, and so $N_{\mathrm{ph}}^{\mathrm{tot}}\sim10^{7}$. As an example consider a 35 mm format Sigma 28–300 mm/F3.5–6.3 lens[22] with a depth of field of about 40–60 cm at a 50 cm distance (for all focal lengths and aperture settings) and a variable field of view (FOV) of 8°–75°. Assume that a dust tail has a cigar shape with 10×2 mm^2 characteristic dimensions, and that it is parallel to the long dimension of the lens image area (36×24 mm^2). Then the tail will be focused onto 60×12 (for FOV ~60°) or 410×82 (for FOV ~10°) fibers. A lens system then relays the image from 1500×1200 fibers onto 1280×1024 pixels of the camera, so every 1.17×1.17 fibers fill out one pixel. Assume now that at each focal length (FOV) setting the lens is used at the maximum permissible aperture setting, so that 90% or more (depending on the internal properties of the lens) of the light reaching its front surface is focused onto the image plane. In view of the above, the total number of photons received by each pixel during one exposure can be estimated as $N_{\mathrm{ph}}^{\mathrm{tot/pix}}\sim4\times10^{2}-2\times10^{4}$. Comparing it to the number of photons from plasma bremsstrahlung radiation, we estimate a signal-to-noise ratio (SNR) $\sim10^{4}$, with the 10 nm bandwidth, 427 nm C I filter in place, and SNR ~250 without the filter. Since $N_{\mathrm{ph}}^{\mathrm{tot}}(\mathrm{dust})\propto T_{e0}^{3/2}$ and $N_{\mathrm{ph}}^{\mathrm{tot}}(\mathrm{plasma})\propto T_{e0}^{-1/2}$, for a plasma with $T_{e0}=100$ eV, we obtain SNRs $\sim10^{2}$ and 2.5, respectively.

III. IMAGING SYSTEM TESTING ON NSTX

Figure 1 shows the schematic drawing of the prototype imaging system deployed on NSTX in 2005. A C-mount 6.5 mm/F1.8 fisheye fixed focus lens was placed in front of the 5.7 cm window at Bay K. It surveyed the right half-torus and the center stack of the machine, to photograph pellet ablation clouds from behind. The camera was situated approximately 4 m from Bay K. It was triggered by a TTL-level signal synchronized with the machine clock. The camera was coupled to the fisheye lens via a 5 m 1000×800 coherent fiber bundle (Schott Fiber Optics, Inc.) made out of 10×10 μm^2 fibers. A Navitar 25 mm/F0.95 variable focus lens was C mounted onto the fiber bundle and a Nikon 50 mm/F1.4 lens was F mounted onto the camera. Both lenses were focused approximately at infinity to relay the image from the fiber bundle onto the CCD. The fisheye and Navitar lenses were fully open, and the Nikon lens was used at $F=2$. No interference filter was used. The camera was placed inside a 15 cm wide, 20 cm tall, and 60 cm long iron enclosure with a 0.64 cm thick wall, so that estimated magnetic field in the center of the enclosure (where the CCD was located) was below 100 G.

Figure 3 shows the photographs taken during high beta-poloidal shots 116056 and 116059. Note a bright, sharp, and distinctively concave inner plasma edge. Also interesting are the bright "filaments"—plasma cords with very high density and temperature.[6] They cross the bulk plasma and twirl around the center stack in both top and bottom portions of the machine.

Figure 4 shows lithium pellet ablation cloud photographed during pellet shot 117028. Pellet velocity was 150 m/s, and its mass was 5 mg. Pellets are much slower than hypervelocity dust particles, and thus cannot be used to determine central magnetic field distribution. Their penetration length into NBI heated discharges can be estimated as ~20 cm. A second dedicated camera is required to measure the pellet's radial position. Pitch angle calculation from EFIT_02 simulation program[20] corresponds closely to the measured value for the Li pellet ablation cloud. This confirms the feasibility of this technique to measure B-field angle in the outer 20 cm of NSTX, from which edge q can be derived.

ACKNOWLEDGMENTS

The authors wish to thank Tom Holoman for his help with preparation of the experiments. This work was supported by DOE Contract Nos. W-7405-ENG-36 and DE-ACO2-76CHO3073, and the Los Alamos Laboratory Directed Research and Development (Exploratory Research program).

[1] G. A. Wurden, K. Büchi, J. Hofmann, R. Lang, R. Loch, A. Rudyj, and W. Sandmann, Rev. Sci. Instrum. **61**, 3604 (1990).
[2] R. J. Maqueda and G. A. Wurden, Nucl. Fusion **39**, 629 (1999).
[3] R. J. Maqueda, G. A. Wurden, J. L. Terry, and J. Gaffke, Rev. Sci. Instrum. **72**, 927 (2001).
[4] C. J. Boswell, J. L. Terry, B. Lipschultz, and J. Stillerman, Rev. Sci. Instrum. **72**, 935 (2001).
[5] A. Huber *et al.*, Proceedings of the 30th EPS Conference on Controlled Fusion and Plasma Physics, St. Petersburg, Russia, 2003, ECA Vol. 27A, p. 3.199.
[6] S. J. Zweben *et al.*, Nucl. Fusion **44**, 134 (2004).
[7] A. L. Roquemore, T. Biewer, D. Johnson, S. J. Zweben, N. Nishino, and V. A. Soukhanovskii, Rev. Sci. Instrum. **75**, 4190 (2004).
[8] I. Furno, T. P. Intrator, E. W. Hemsing, S. C. Hsu, S. Abbate, P. Ricci, and G. Lapenta, Phys. Plasmas **12**, 055702 (2005); www.cookecorp.com
[9] Z. Wang *et al.*, Rev. Sci. Instrum. **76**, 033501 (2005).
[10] TFR Group, Nucl. Fusion **27**, 1975 (1987).
[11] Z. Wang and G. A. Wurden, Rev. Sci. Instrum. **74**, 1887 (2003).
[12] Z. Wang and G. A. Wurden, Rev. Sci. Instrum. **75**, 3436 (2004).
[13] Z. Wang, C. M. Ticos, L. A. Dorf, and G. A. Wurden, IEEE Trans. Plasma Sci. **34**, 242 (2006).
[14] L. Dorf *et al.*, Web Proceedings of the Micro- and Nano-Gadgets: Applications and Fabrications Conference, Santa Fe, NM, 2005 (unpublished) http://wsx.lanl.gov/nano2005_webpages/Presentations/Talks.htm
[15] A. Yu. Pigarov, S. I. Krasheninnikov, T. K. Soboleva, and T. D. Rognlien, Phys. Plasmas **12**, 122508 (2005).
[16] P. K. Shukla and A. A. Mamun, *Introduction to Dusty Plasma Physics* (IOP, Bristol, London, 2002), Chap. 2.
[17] R. E. Bell *et al.*, Proceedings of the 28th EPS Conference on Controlled Fusion and Plasma Physics, Funchal, Portugal, 2001, ECA Vol. 25A, pp. 1021–1024.
[18] M. Ono *et al.*, Nucl. Fusion **41**, 1435 (2001).
[19] R. Maingi *et al.*, Plasma Phys. Controlled Fusion **45**, 657 (2003).
[20] S. A. Sabbagh *et al.*, Nucl. Fusion **41**, 1601 (2001).
[21] www.us.schott.com
[22] www.sigma.com